Am J Physiol Lung Cell Mol Physiol 309: L1186–L1198, 2015.
First published September 4, 2015; doi:10.1152/ajplung.00044.2015.

Maternal-pup interaction disturbances induce long-lasting changes in the newborn rat pulmonary vasculature

Yulia Shifrin,[1] Sina Sadeghi,[1] Jingyi Pan,[1] Amish Jain,[2] Andres F. Fajardo,[1] Patrick J. McNamara,[1,2] and Jaques Belik[1,2]

[1]*Physiology and Experimental Medicine Program, The Hospital for Sick Children Research Institute, Toronto, Ontario, Canada; and* [2]*Department of Paediatrics and Physiology, University of Toronto, Toronto, Ontario, Canada*

Submitted 8 February 2015; accepted in final form 2 September 2015

Shifrin Y, Sadeghi S, Pan J, Jain A, Fajardo AF, McNamara PJ, Belik J. Maternal-pup interaction disturbances induce long-lasting changes in the newborn rat pulmonary vasculature. *Am J Physiol Lung Cell Mol Physiol* 309: L1186–L1198, 2015. First published September 4, 2015; doi:10.1152/ajplung.00044.2015.—The factors accounting for the pathological maintenance of a high pulmonary vascular (PV) resistance postnatally remain elusive, but neonatal stressors may play a role in this process. Cross-fostering in the immediate neonatal period is associated with adult-onset vascular and behavioral changes, likely triggered by early-in-life stressors. In hypothesizing that fostering newborn rats induces long-lasting PV changes, we evaluated them at 14 days of age during adulthood and compared the findings with animals raised by their biological mothers. Fostering resulted in reduced maternal-pup contact time when compared with control newborns. At 2 wk of age, fostered rats exhibited reduced pulmonary arterial endothelium-dependent relaxation secondary to downregulation of tissue endothelial nitric oxide synthase expression and tetrahydrobiopterin deficiency-induced uncoupling. These changes were associated with neonatal onset-increased ANG II receptor type 1 expression, PV remodeling, and right ventricular hypertrophy that persisted into adulthood. The pulmonary arteries of adult-fostered rats exhibited a higher contraction dose response to ANG II and thromboxane A_2, the latter of which was abrogated by the oxidant scavenger Tempol. In conclusion, fostering-induced neonatal stress induces long-standing PV changes modulated via the renin-angiotensin system.

neonatal stressors; pulmonary vasomotor tone; renin angiotensin system

THE TRANSITION FROM FETAL to postnatal life is characterized by a rapid decrease in pulmonary vascular resistance (PVR), as a result of the birth-associated lung expansion, alveolar oxygenation, and CO_2 removal (58). Infants with the so-called persistent pulmonary hypertension syndrome of the newborn (PPHN) either fail to show the physiological decline in PVR at birth or exhibit a postnatal increase in resistance (19). Neonatal stressors as one of the causative factors of this syndrome have been suggested (57), but their pathogenesis is poorly understood.

The renin-angiotensin (Ang)-aldosterone system (RAAS) plays an essential role in systemic blood pressure regulation and is a likely modulator of the stress-induced vasomotor tone. RAAS primarily depends on the renal cell generation of renin, which in turn, promotes the liver and fat-derived angiotensinogen conversion to ANG I. Ang-converting enzyme (ACE), mostly present in the lungs, converts ANG I into the vasoactive form ANG II that signals through two main receptors: ANG II receptor types 1 and 2 (AT_1 and AT_2, respectively) (42). In the regulation of vascular resistance, AT_1 receptors are responsible for vasoconstriction and vessel-wall compliance, whereas AT_2 receptors modulate vasodilation (25, 49, 51, 52). Adding to the renin-angiotensin system complexity, ACE2 promotes the conversion of ANG II into Ang-(1–7), which induces vasodilation via the Mas receptor (24). Downregulation of Ang-(1–7) and/or its Mas receptor is associated with systemic hypertension (24).

A prenatal, maternal low-protein diet results in late-onset systemic hypertension in rats via a mechanism involving RAAS (32, 34). This fetal programming is characterized by an enhanced vasomotor response to ANG II later in life, secondary to the increased renal and vascular tissue AT_1 receptor expression (65). Such fetal programming is not limited to the systemic circulation, since a restrictive protein diet during gestation also induces an increase in lung ACE activity in adult mice (62).

Fetal sheep delivered by cesarean section have lower plasma ANG II levels when compared with animals born vaginally (11), suggesting that birth-related stress is associated with higher concentration of this metabolite in the immediate neonatal period. Limited studies, however, previously addressed the impact of postnatal stressors on the regulation of vascular tone. Maternal cross-fostering in the early postpartum period in rodents is associated with adult-onset systemic hypertension and metabolic dysfunction (43), as well as behavioral abnormalities (40). Changes in maternal pup-rearing behavior in rodents are known to promote neonatal humoral changes that result in altered stress response later in life (27). Thus there is reason to suspect that maternal cross-fostering via maternal-pup interaction disturbances results in neonatal stress. Yet, the mechanism accounting for these changes and whether they are limited to the systemic circulation are presently unknown and the main focus of the present study.

In hypothesizing that maternal cross-fostering promotes neonatal pulmonary vasomotor changes via RAAS, we comparatively evaluated control and fostered rat pups in the immediate postnatal period and later in life. The maternal behavior following cross-fostering was assessed continuously during the 1st wk postpartum, and the factors potentially affecting the pulmonary vasomotor regulation were evaluated. Cross-fostering promotes RAAS-dependent endothelial dysfunction, which results in short- and long-term PV changes.

MATERIALS AND METHODS

Animals

Time-bred Sprague-Dawley rats were studied from birth until adulthood. All procedures were conducted according to criteria established by the Canadian Council on Animal Care and were approved by

Address for reprint requests and other correspondence: J. Belik, The Hospital for Sick Children Research Institute, 555 University Ave., Toronto, Ontario, M5G 1X8, Canada (e-mail: jaques.belik@sickkids.ca).

the Animal Care Committee of The Hospital for Sick Children Research Institute.

Cross-Fostering and Maternal Behavior Monitoring

Cross-fostering. Female rats were bred and their litters culled to 12 pups, randomly assigned in the immediate postpartum period to be either raised by their biological mothers (control group) or by a foster doe. Cross-fostering was conducted as follows: two female rats were time bred such that their litters were born within <24 h of each other. On the morning of the second postpartum day, the mothers were swapped, such that they were no longer raising their biological pups. Daily pup body weight was obtained during the first 14 days of life by placing each pup on a laboratory scale with a 0.1-g precision accuracy. The mother and litter were maintained in a 12-h timed light-dark cycle quiet room, and the cages were cleaned twice/week. The mothers were fed a regular pellet diet, and water was provided ad libitum.

Maternal behavior. In a subset of animals, maternal behavior was videotaped continuously for the first 7 postpartum days. Footage was recorded continuously using two cameras positioned at different angles to ensure constant maternal-behavior tracking. The recorded videos were later scored by one of the investigators (S. Sadeghi) without knowledge of the group assignment. Maternal behavior was scored, as proposed by others (14), in one of five categories and the precise duration of each category recorded. The distinct maternal behavior categories used in this study were as follows: *1*) arched-back nursing; *2*) blanket nursing (laying over the pups in a blanket position; *3*) passive nursing (passive nursing while in a supine or side position); *4*) grooming the pups; *5*) no pup contact. The distinct maternal behaviors are reported as a percentage of the total observation time over a 24-h period.

Organ Bath Studies and Fulton Index Determination

The rats were studied at 7, 14, and 60–90 (adult) days of age. The animals were euthanized with an overdose of pentobarbital sodium (50 mg/kg ip). The lungs were quickly removed and maintained on an ice bed; the heart was excised and maintained in 4% buffered paraformaldehyde for future determination of the Fulton index.

The near-resistance (third to fourth generations) intrapulmonary arteries were dissected free and mounted on a wire myograph (Danish Myo Technology A/S, Aarhus, Denmark). The muscle bath was filled with Krebs-Henseleit buffer solution (NaCl, 115 mM; $NaHCO_3$, 25 mM; $NaHPO_4$, 1.38 mM; KCl, 2.51 mM; $MgSO_4$-7 H_2O, 2.46 mM; $CaCl_2$, 1.91 mM; and dextrose, 5.56 mM), bubbled with air/6% CO_2, and maintained at 37°C. After 1 h of equilibration, the optimal vessel resting tension was determined by repeated stimulation with 128 mM KCl until maximum active tension was reached. All subsequent force measurements were obtained at optimal resting tension.

PV muscle force generation was evaluated by stimulating with the thromboxane A_2 mimetic U46619 or ANG II. Contractile responses were normalized to the tissue cross-sectional area as follows: (width × diameter) × 2, expressed as milli-newtons/square millimeter. The relaxant response to endothelium-dependent acetylcholine and the endothelium-independent nitric oxide (NO) donor S-nitroso-*N*-acetyl-penicilamine were determined after vascular muscle precontraction with U46619 (10^{-6} M).

For the Fulton index determination, the hearts were dissected to obtain the right-ventricular (RV) wall and left-ventricle plus septum weights (4). The data are expressed as the RV/left-ventricular plus septum-weight ratio and used as a measure of RV hypertrophy.

Western Blot Analysis

Vascular endothelial cells were isolated from freshly dissected peripheral lung tissue by digesting with 1 mg/ml collagenase type II (Sigma-Aldrich, Oakville, Ontario, Canada) for 2 h at 37°C. The digest was then passed through a 70-μm cell strainer to remove tissue fragments, pelleted by centrifugation at 200 G for 10 min, and resuspended with 2% FBS (Gibco, Ontario, Canada) in PBS containing 5 μl biotinylated rat anti-mouse CD31 antibody (BD PharMingen, San Diego, CA). After incubation on ice for 1 h, the endothelial cells were immobilized with streptavidin magnetic beads (New England BioLabs, Ipswich, MA). The endothelial cells were then placed on the EasySep magnet (Stemcell Technologies, Vancouver, BC, Canada) for 5 min and the unbound cells removed. Bead-bound endothelial cells were lysed in 10 mmol/l Tris-HCl, pH 7.4, lysis buffer containing 1% Triton X-100 and protease/phosphatase inhibitors (Roche Diagnostics Canada, Laval, Quebec, Canada) and centrifuged at 13,000 *g* for 30 min. Protein content was determined by the Bradford method using the Bio-Rad protein assay (Bio-Rad Laboratories, Hercules, CA).

Equal amounts of lysate proteins in Laemmli buffer were separated by SDS-PAGE, transferred onto polyvinylidene fluoride membrane, and immunoblotted using the following antibodies: mouse endothelial NO synthase (eNOS; 1:1,000; BD Biosciences, Franklin Lakes, NJ), mouse dihydrofolate reductase (DHFR; 1:1,000; Cell Signaling Technology, Danvers, MA), mouse tubulin (1:5,000; Santa Cruz Biotechnologies, Santa Cruz, CA), anti-mouse IgG horseradish peroxidase (HRP) conjugated (1:10,000; Sigma-Aldrich), and anti-rabbit IgG HRP conjugated (1:5,000; Cell Signaling Technology). Detection was performed with the enhanced chemiluminescence reagent (PerkinElmer, Waltham, MA). Band intensities were quantified using ImageJ software (National Institutes of Health, Bethesda, MD) and expressed relative to tubulin. Cell lysates from control and cross-fostered animals were run on the same gel for comparison, and nonessential lanes were removed during image processing.

eNOS Dimer/Monomer Ratio

To ascertain for the eNOS coupling state, lung tissue was dissected and homogenized immediately in cold lysis buffer containing 10 mmol/l Tris-HCl, pH 7.4, 1% Triton X-100, and protease/phosphatase inhibitors without boiling and separated on 4% lithium dodecyl sulfate-PAGE maintained at 4°C. Proteins were immunoblotted using eNOS antibody, as above described. The ratio of dimer over monomer expression was determined by measuring the Western blot-respective band densities using ImageJ software.

Lung H_2O_2 Content

The lung tissue H_2O_2 content was measured as a surrogate marker of superoxide generation. For this, lung tissue was homogenized in cold lysis buffer, followed by centrifugation at 13,000 *g* for 30 min, and divided into two groups. For the first group, the lysate H_2O_2 content was determined by the Amplex Red Hydrogen Peroxide/Peroxidase Assay Kit (Life Technologies, Carlsbad, CA), according to the manufacturer's protocol. The second group of tissue homogenates was first preincubated with polyethylene glycol-superoxide dismutase (PEG-SOD; 250 U/ml) for 30 min. Absorbance of all samples was measured at ~560 nm using POLARstar Omega microplate reader (BMG LABTECH, Ortenberg, Germany). The difference between the absorbance of PEG-SOD-treated and untreated samples represents SOD-inhibitable H_2O_2 tissue content. Tissue total protein was determined by the Bradford method using the Bio-Rad protein assay (Bio-Rad Laboratories) and used for data normalization.

Table 1. *Primers used for the RT-PCR assays*

Target	Oligonucleotide Sequence
AT_1	F: CTCAAGCCTGTCTACGAAAAT GAG
	R: TAGATCCTGAGGCAG GGTGAAT
AT_2	F: ACCTTTTGAACATGGTGCTTTG
	R: GTTTCTCTGGGTCTGTTTGCTC
MAS	F: TGTGGGTGGCTTTCGATTT
	R: ATTAGACCCCCATGCATGTAGAA
ACE	F: CAGCTTCATCATCCAGTTCC
	R: CTAGGAAGAGCAGCACCCAC
NOX1	F: TGAACAACAGCACTCACCAATGCC
	R: AGTTGTTGAACCAGGCAAAGGCAC
NOX2	F: CCAGTGAAGATGTGTTCAGCT
	R: GCACAGCCAGTAGAAGTAGAT
NOX4	F: ACCAGATGTTGGGCCTAGGATTGT
	R: AGTTCACTGAGAAGTTCAGGGCGT
GAPDH	F: CCCTTCATTGACCTCAACTACATG
	R: CTTCTCCATGGTGGTGAAGAC

$AT_{1/2}$, ANG II receptor types 1/2; ACE, angiotensin-converting enzyme; NOX1/2/4, NADPH oxidase 1/2/4; F, forward; R, reverse.

Lung ROS Generation

Lung tissue homogenates were divided into two groups. Lucigenin was added to the first group of samples to a final concentration of 5 mM, and 50 ml of the homogenate-lucigenin mixture was transferred to individual wells of an opaque, white 384-well plate. To confirm further the specificity of the measurement for superoxide determination, the second group of tissue homogenates was preincubated with 0.1 mM N^G-nitro-L-arginine methyl ester (L-NAME) for 30 min at 37°C before adding lucigenin. The reaction was started by the addition of 100 mM NADPH. Chemiluminescence readings were recorded every 3 min over a period of 30 min in a POLARstar Omega microplate reader (BMG LABTECH). Background signals from buffer were subtracted from homogenate signals, and the resulting value was further corrected by determining the L-NAME-inhibitable values and normalized for protein concentration.

Real-Time qPCR

Total RNA was isolated from lung tissue using the PureLink RNA Mini Kit (Life Technologies), according to the manufacturer's instructions. First-strand cDNA was synthesized from 1 μg RNA by Superscript II RT (Life Technologies) and amplified by real-time quantitative (q)PCR using SYBR Select Master Mix (Life Technologies). Primers used are listed in Table 1. For quantification, mRNA expression of the target gene was normalized to the expressed housekeeping gene GAPDH.

Biopterin Measurements

Tissue biopterin concentrations were determined by liquid chromatography electrospray tandem mass spectrometry. A triple quadrupole mass spectrometer API 4000 (Applied Biosystems/MDS SCIEX, Foster City, CA), operated in negative ionization mode with the TurboIonSpray ionization probe source and coupled to an Agilent 1100 HPLC system (Agilent Technologies, Palo Alto, CA), was used. The method used a C_{18} column (150 × 2 mm id, 5 μm particle size, 110 Å pore size) with an isocratic solvent system of water with 0.002% formic acid at 0.3 ml/min and a run time of 13 min. Tissue tetrahydrobiopterin (BH4) and dihydrobiopterin (BH2) concentration were measured after differential iodine oxidation, as described previously (63).

Echocardiographic Assessment of PVR Changes

The inverse ratio of pulmonary arterial acceleration time (PAAT) to RV ejection time (RVET), as a surrogate of PVR, was measured by two-dimensional echocardiography/Doppler ultrasound, as described previously in detail (5, 22, 23). Briefly, a short axis view at the level of the aortic valve was obtained, and the pulmonary artery was identified using color-flow Doppler. The PAAT was measured as the time from the onset of systolic flow to peak pulmonary outflow velocity and the RVET as the time from onset to completion of systolic pulmonary flow.

Tricuspid annular plane systolic excursion (TAPSE) was measured by M-mode. An M-mode cursor was oriented to the junction of the tricuspid valve annulus and the RV free wall, using the apical four-chamber view. TAPSE was measured as the perpendicular distance covered by the tricuspid annulus in systole in adult rats. For technical reasons, TAPSE measurement cannot be obtained in the newborn rat. Measurements were obtained and averaged for three consecutive cardiac cycles. This parameter has been shown by others to be a very robust measurement of RV dysfunction in the rat model of pulmonary hypertension and is used routinely in clinical practice (9, 32, 37).

Lung histology. A subset of 14-day-old and adult animals from both groups was prepared for lung histology, as we have described previously (26). Briefly, the lungs were inflated with 4% paraformaldehyde at a constant pressure (20 cm H_2O) and the PV perfused with heparinized physiologic buffer saline at an average pressure of 30 mmHg and paraffin embedded. A 4-μm section was cut and stained with Masson's trichrome to allow for clear demarcation of the internal and external elastic lamina, as well as the muscle layer. With the aid of a computerized image analyzer system (Openlab/Improvision, PerkinElmer), coupled with a fine-resolution microscope, the external and internal perimeters of each identifiable pulmonary artery were measured. The arterial lumen diameter was calculated as internal perimeter/π. The arterial muscle layer was quantified by measuring the medial area (external-internal arterial area in square millimeters).

Statistical Methods

Data were first evaluated to determine Gaussian distribution by Skewness, Kurtosis, and Omnibus testing. Normally, distributed data were analyzed by repeated-measures, two-way ANOVA with multiple comparisons obtained by the Tukey-Kramer test or unpaired Student's *t*-test when appropriate. The Mann-Whitney *U*-test was used for nonparametric data. Statistical significance was determined at $P < 0.05$. All statistical analyses were performed with the Number Cruncher Statistical System software (NCSS, Kaysville, UT). Data are presented as means ± SE.

RESULTS

Cross-Fostering Affects Maternal-Newborn Interaction

Cross-fostering had no impact on the experimental pups' breast-milk intake, as judged by the nonsignificant differences

Table 2. *Pup body weight at 7 and 14 days of age for control and experimental groups*

	Control	Fostered
14 Days		
Body weight, g	27.9 ± 0.4 (24)	27.7 ± 0.7 (35)
RV/body weight, $\times 10^{-3}$	1.00 ± 0.03 (8)	1.18 ± 0.03 (10)*
LV + sept/body weight, $\times 10^{-3}$	3.12 ± 0.08 (8)	3.54 ± 0.06 (10)†
Adult		
Body weight, g	219 ± 8 (41)	241 ± 5 (61)†
RV/body weight, $\times 10^{-3}$	6.63 ± 0.02 (8)	7.76 ± 0.02 (10)*
LV + sept/body weight, $\times 10^{-3}$	2.37 ± 0.05 (8)	2.71 ± 0.05 (10)*

Values are means ± SE (number of pups). RV, right ventricular; LV, left ventricular; sept, septum. *$P < 0.01$ and †$P < 0.05$ compared with control animal values.

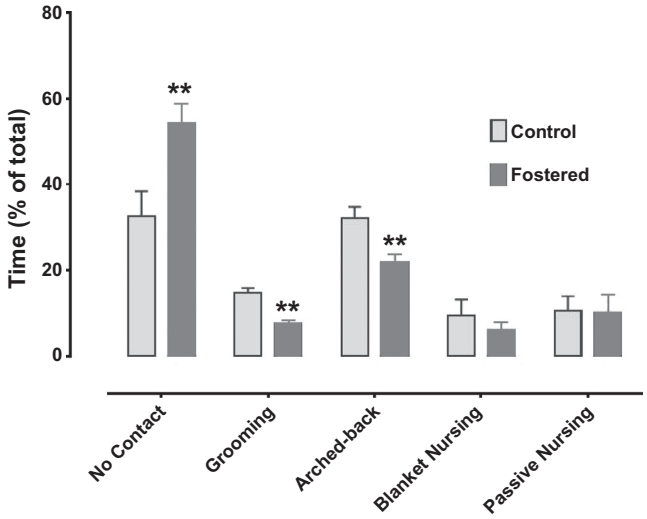

Fig. 1. Cross-fostering effect on the maternal-pup interaction. Maternal behavior during the 72-h postcross-fostering ($n = 3$) or equivalent period for controls ($n = 4$) was determined by continuous video monitoring and offline scoring. Methodological details are provided in the text. Means ± SE. $^{**}P < 0.01$ compared with control group by unpaired Student's *t*-test.

in pups' body weight at 14 days of life (Table 2). Yet, significant changes in maternal-pup interaction were documented in fostered litters. As shown in Fig. 1, during the first 72-h postcross-fostering initiation, the experimental pups experienced significantly less maternal contact and grooming when compared with animals raised by their biological mothers.

Cross-Fostering Induces Early-Onset PV Endothelium-Dependent Changes

We next evaluated the cross-fostering effect on the RV wall mass by comparatively measuring the Fulton index at 14 days of age (Fig. 2*A*) and later in adulthood (Fig. 2*B*). At both ages, fostered pups exhibited higher index values when compared with same-age control animals. The RV/body weight ratio was also increased significantly in fostered when compared with control animals of both ages (Table 2). No sex-dependent group differences in either the Fulton index or RV/body weight ratio were observed. Lastly, the left ventricular + septum/body weight ratio was increased in the experimental animals when compared with control rats of both ages (Table 2).

Echocardiographic PVR assessment showed no group differences for 14-day-old and adult animals (Fig. 3, *A* and *B*, respectively). Adult-fostered rats, however, exhibited a significant reduction in TAPSE, indicative of RV dysfunction, when compared with same-age control animals (Fig. 3*C*), possibly accounting for the lack of group difference in PVR index later in life. The TAPSE measurement is not technically feasible at 2 wk of age.

The pulmonary arterial medial smooth muscle mass was evaluated in control and fostered animals at 14 days of age and during adulthood (Fig. 4). At both ages, the fostered group's mid-size and large diameter pulmonary arterial muscle mass was increased significantly when compared with control animals.

To evaluate the factors accounting for the cross-fostering effect on the pulmonary vasculature, we proceeded to study the animals' pulmonary arterial smooth muscle contraction and relaxation potentials. Following agonist-induced contraction, a significant age-dependent group difference in dose response was observed (Fig. 5, *A* and *B*). Whereas no group differences were observed at 14 days of age (Fig. 5, *A* and *C*), adult pulmonary arteries exhibited a significantly increased ($P < 0.01$) dose response to ANG II and thromboxane A_2 analog U46619 when compared with control animals (Fig. 5, *B* and *D*). Tempol, a reactive oxygen species (ROS) scavenger, reduced the fostered adult animals' U46619-induced dose response to a level comparable with control rat values (Fig. 5*E*).

A distinct age-dependent difference in pulmonary arterial relaxation potential was also observed between groups (Fig. 6). Compared with vessels from control-group animals, endothelium-dependent pulmonary arterial relaxation dose response was reduced significantly in 14-day-old fostered pups (Fig. 6*A*) but not adult animals (Fig. 6*C*). There was no significant group differences in endothelium-independent pulmonary arterial relaxation response at either age (Fig. 6, *B* and *D*).

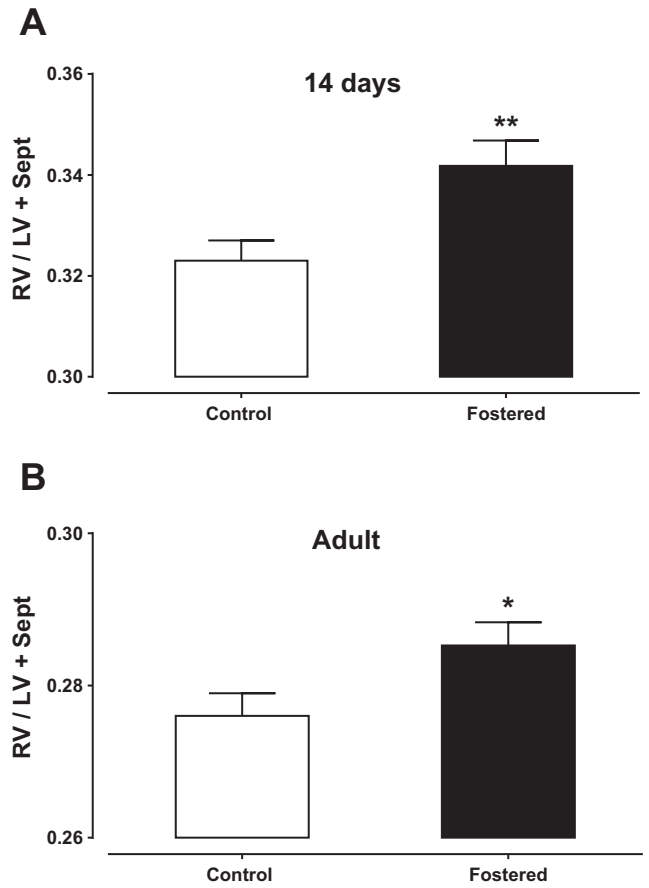

Fig. 2. Fulton index for control and fostered animals. The right ventricular/left ventricular + septum ratio (RV/LV + Sept) was measured in control and fostered animals at 14 days of life (*A*; $n = 20$ and 21, respectively) and during adulthood (*B*; $n = 33$ and 50, respectively). Means ± SE. $^{**}P < 0.01$ and $^{*}P < 0.05$ compared with age-matched control animals by unpaired Student's *t*-test.

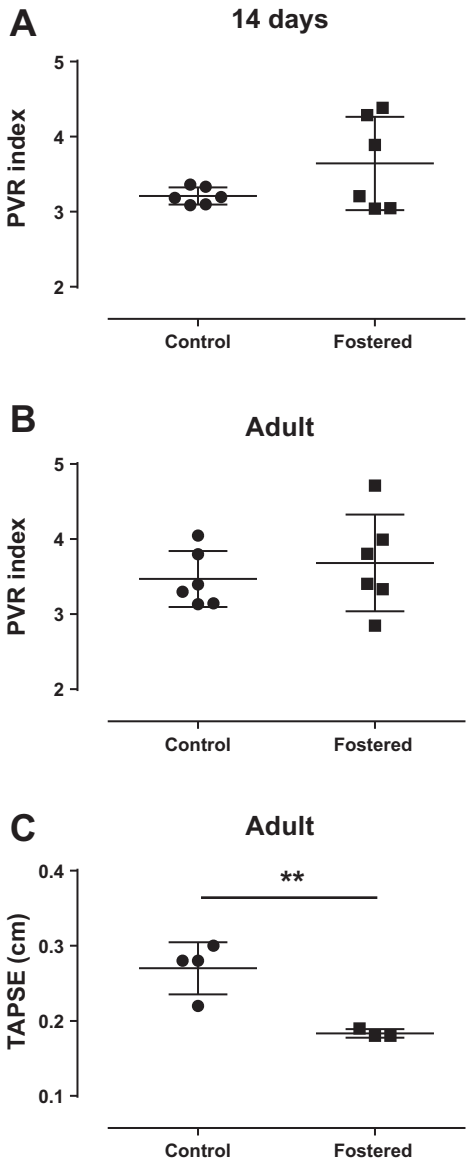

Fig. 3. Echocardiographic measurements. The pulmonary vascular resistance (PVR) index for control and fostered animals at 14 days of age (*A*; $n = 6$ for both groups) and adults (*B*; $n = 6$ for both groups) is shown, together with the tricuspid annular plane systolic excursion (TAPSE; *C*; control, $n = 4$; fostered, $n = 3$) in adult rats. $^{**}P < 0.01$ compared with control values. See methodology for detailed description of echocardiographic measurements.

Fostering Is Associated with Lung eNOS Expression Downregulation and Uncoupling, As Well As Increased ROS Generation

Given the abnormal endothelium-dependent pulmonary arterial relaxation response of 14-day-old fostered pups, we proceeded to investigate the mechanism responsible for this change. We first hypothesized that cross-fostering may induce age-dependent changes in lung vascular endothelial cell eNOS expression and/or uncoupling. Indeed, a marked decrease in lung endothelial cells' eNOS expression was documented in fostered animals at 2 wk of age but not later in adulthood when compared with control group animals (Fig. 7).

We further evaluated the lung tissue ROS generation for control and fostered animals at both ages. When compared with control animals, a 14-fold increase in lung H_2O_2 content was documented in the 2-wk fostered pups, whereas no group difference was observed in adult animals (Fig. 8*A*). To confirm further that cross-fostering enhanced eNOS-dependent lung ROS generation, we measured tissue total and L-NAME-inhibitable superoxide levels at both ages using the lucigenin chemiluminescence assay (Fig. 8*B*). Compared with control animals, total chemiluminescence values were increased significantly in fostered animals at both ages. Yet, an L-NAME-inhibitable, lucigenin-derived signal was significantly higher in fostered pups at 14 days of age but not during adulthood.

These data led us to interrogate whether eNOS uncoupling was responsible for the increased ROS generation in fostered pups. Compared with control pups, the eNOS dimer/monomer

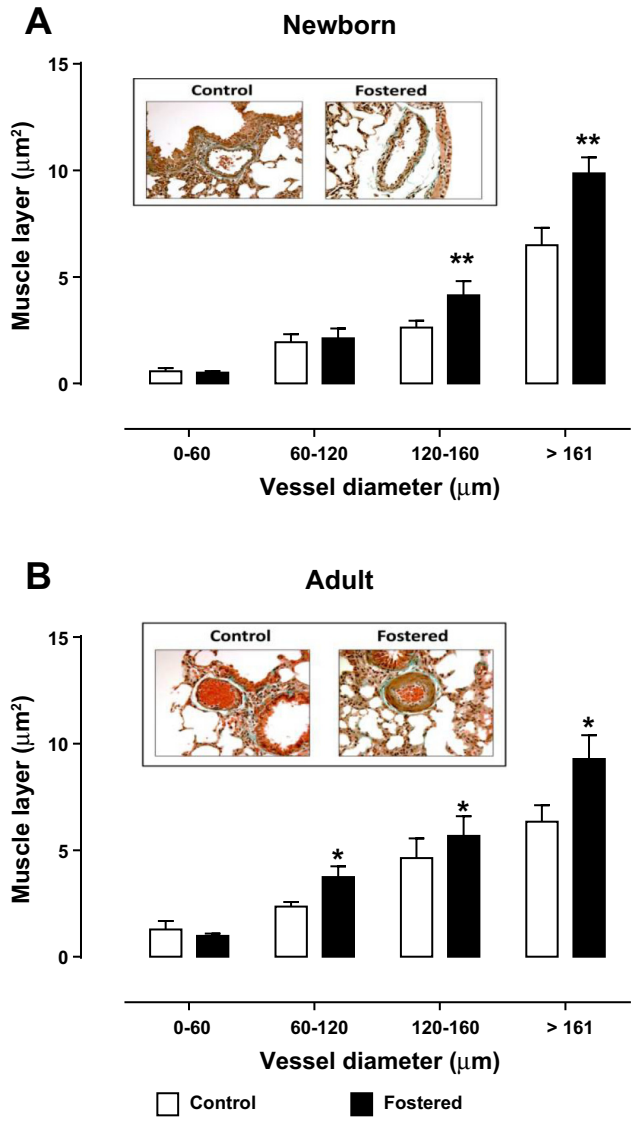

Fig. 4. PV remodeling. Pulmonary arterial muscle layer area from 14 days of age and adult control ($n = 5$ and 3, respectively) and fostered ($n = 4$ for both ages) animals for vessels of different diameters ($n > 10$ for each diameter/group). $^{*}P < 0.05$ and $^{**}P < 0.01$ compared with control values. *Insets*: typical mid-size diameter pulmonary arteries of control and fostered animals of both ages.

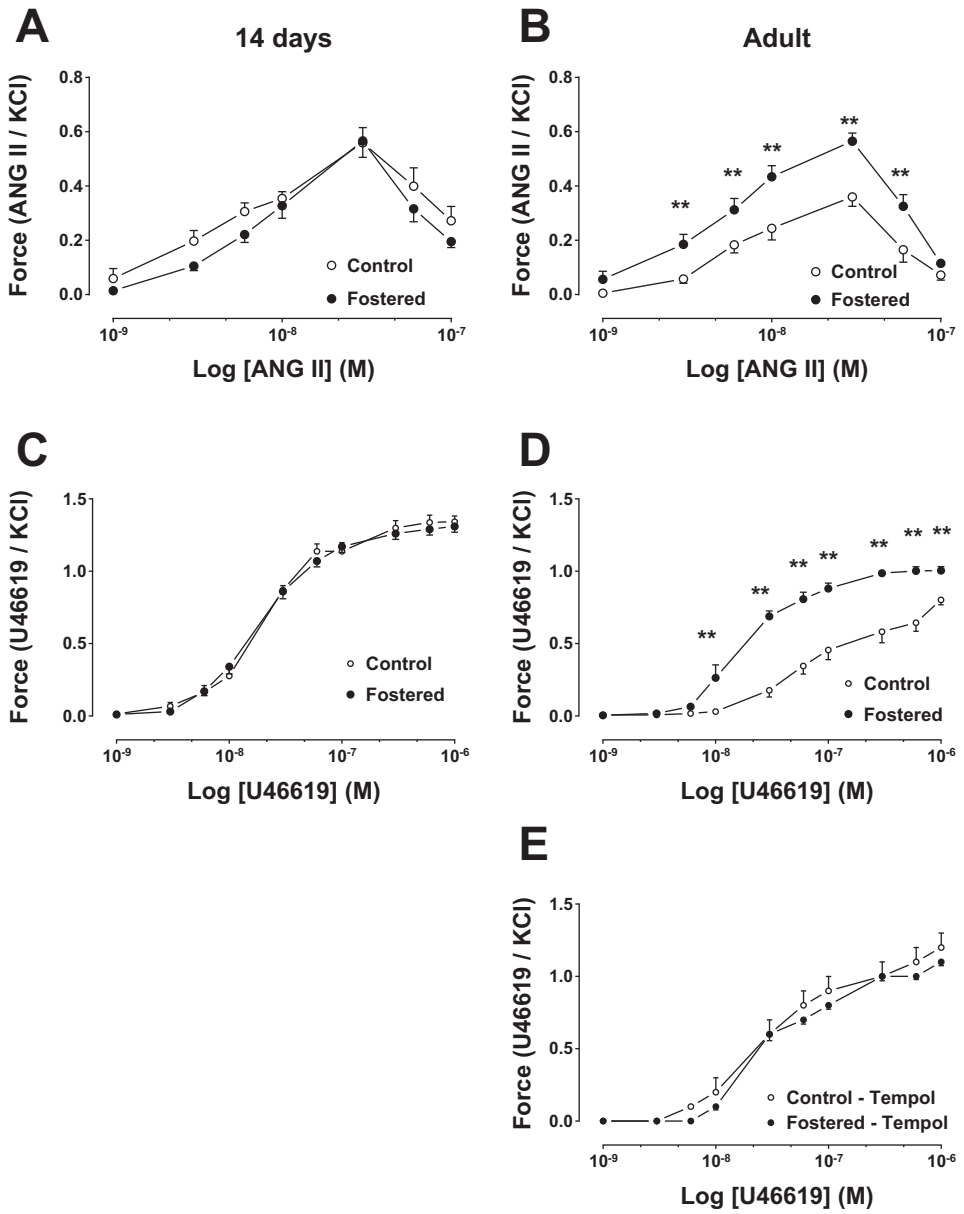

Fig. 5. Pulmonary vasomotor contraction. Vasocontraction dose response in near-resistance pulmonary arteries from control and fostered 14-day-old (n = 18 and 12, respectively) and adult (n = 12 and 4) induced by ANG II (*A* and *B*) and thromboxane A_2 analog (U46619; *C* and *D*). Tempol (10^{-3} M) preincubation normalized the U46619-induced dose response of the adult-fostered animals (*E*; n = 8 for both groups). Data expressed as means ± SE and normalized to the response to 120 mM KCl. $^{**}P < 0.001$ compared with control animals by 2-way ANOVA and Tukey-Kramer multiple comparison testing.

ratio, a marker of eNOS uncoupling, was reduced significantly at 14 days of age in fostered animal (Fig. 9*A*).

Fostering-Induced eNOS Uncoupling Is Related to DHFR-Dependent BH4 Deficiency

Amongst other factors, reduced BH4 availability promotes eNOS uncoupling (17). To test whether cross-fostering-induced eNOS uncoupling was related to BH4 deficiency, we determined the lung tissue BH4/BH2 content ratio at 14 days of age in both groups. The lung BH4/BH2 ratio was significantly lower ($P < 0.05$) in fostered pups when compared with control animals at 2 wk of age (Fig. 9*B*), indicating tissue BH4 deficiency.

Since DHFR expression regulates tissue BH4/BH2 ratio by recycling BH2 into BH4 (33), we proceeded to interrogate whether the fostering-induced lung BH4/BH2 ratio changes were the result of a reduction in the PV endothelium DHFR content. Two-week-old fostered pups had significantly ($P < 0.01$) lower DHFR levels in lung vascular endothelial cells when compared with same-age control animals (Fig. 10*A*), whereas no significant group differences were found in adult animals (Fig. 10*B*).

Cross-Fostering Is Associated with Changes in RAAS Components Expression

Based on the previously reported RAAS involvement in the programming of systemic hypertension in rodents (47), we investigated whether a similar mechanism was operative in fostering-induced PV changes. Firstly, we evaluated mRNA expression of the ANG II receptors AT_1 and AT_2 and MAS. When compared with control animals, AT_1 mRNA expression was increased significantly in fostered pups at 14 days of age and during adulthood (Fig. 11, *A* and *B*, respectively), whereas no group differences in AT_2 (Fig.

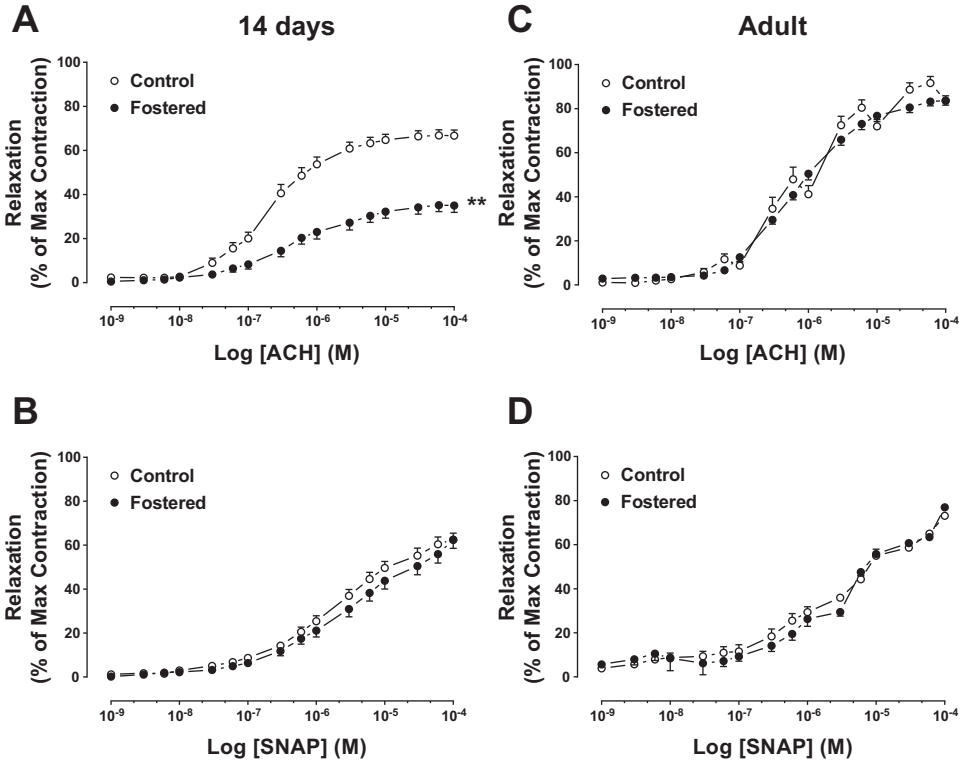

Fig. 6. Pulmonary vasomotor relaxation. Endothelium-dependent [acetylcholine (ACH); *A* and *C*] and -independent [S-nitroso-*N*-acetyl-penicilamine (SNAP); *B* and *D*] vasorelaxation dose response in U46619 precontracted near-resistance pulmonary arteries from control and fostered 14-day-old ($n = 14$ and 18, respectively) and adult ($n = 12$ for both groups) animals. Data expressed as means ± SE. $^{**}P < 0.001$ compared with control animals by 2-way ANOVA and Tukey-Kramer multiple comparison testing.

11, *C* and *D*) or MAS (Fig. 11, *E* and *F*) mRNA expression were documented.

Possibly responsible for the fostering-induced lung AT_1 receptor upregulation was a decrease in its tissue ANG II content. Since the lung ANG II levels are dependent on the expression/activity of ACE, we proceeded to measure the enzyme expression. The lung ACE mRNA expression was reduced significantly in fostered animals at 7 but not 14 days of age when compared with control pups (Fig. 12).

Given the ROS scavenger (Tempol) effect at reducing the U46619-induced, dose-response magnitude in fostered rats to a level comparable with control animals, we speculated whether the NADPH oxidase (NOX) pathway was involved in the increased ROS generation in the experimental group. We documented that NOX1, -2, and -4 isoforms of mRNA expression were increased significantly in adult-fostered animals' lungs when compared with control rat values (Fig. 13), suggesting that this pathway plays a role in fostering-induced ROS generation.

DISCUSSION

In the present study, we showed that cross-fostering results in a significant reduction in maternal-pup contact without affecting the animals' breast-milk intake and weight gain during the first 2 wk of life. Fostered animals exhibited PV changes and RV hypertrophy at 2 wk of age that persisted into adulthood. The factors responsible for the fostering-induced PV changes involve RAAS and are age dependent. Fourteen-day-old fostered pups showed increased ROS generation and impaired eNOS-dependent pulmonary vasodilation secondary to reduced eNOS expression and BH4 deficiency-induced enzyme uncoupling. These changes were associated with a transient decrease in lung ACE expression at 1 wk of age and AT_1 receptor expression upregulation from 14 days until adulthood. Functionally, an increased pulmonary vasomotor response to U46619 and ANG II was documented later in life in fostered animals, and ROS scavenging normalized the U46619-induced enhanced vasocontraction. Lastly, PV remodeling changes were present in fostered animals at 14 days of age and during adulthood.

There is evidence that adverse intrauterine conditions increase the risk of cardiovascular disease in humans (46, 47). Although the mechanism responsible for these changes is poorly understood, RAAS has been implicated in the fetal programming of late-onset systemic hypertension (8, 46). In newborn rodents, maternal separation-induced stress results in attenuation of the hypercapnia response (21), alterations in the hypothalamic-pituitary-adrenocortical axis (7), behavioral changes (30), and ANG II-mediated, adult-onset systemic hypertension (39). Limited studies, however, addressed the effect of neonatal stressors on the pulmonary vasculature.

Maternal pup-rearing behavior is known to modulate behavioral and hemodynamic regulation later in life in rodents (15, 43). In the present study, we showed that cross-fostering in the immediate postpartum period resulted in reduced maternal-pup interaction when compared with the animals reared by their biological mothers. We here propose that the neglect-like behavior exhibited by fostered mothers induced a significant neonatal stress that resulted in PV changes within the first 14 days of life that persisted until adulthood.

The RAAS pathway is developmentally regulated and thus susceptible to early-life stressors. The newborn ANG II plasma levels are highest immediately after birth and gradually decrease afterwards in humans (44) and other mammals (20, 50,

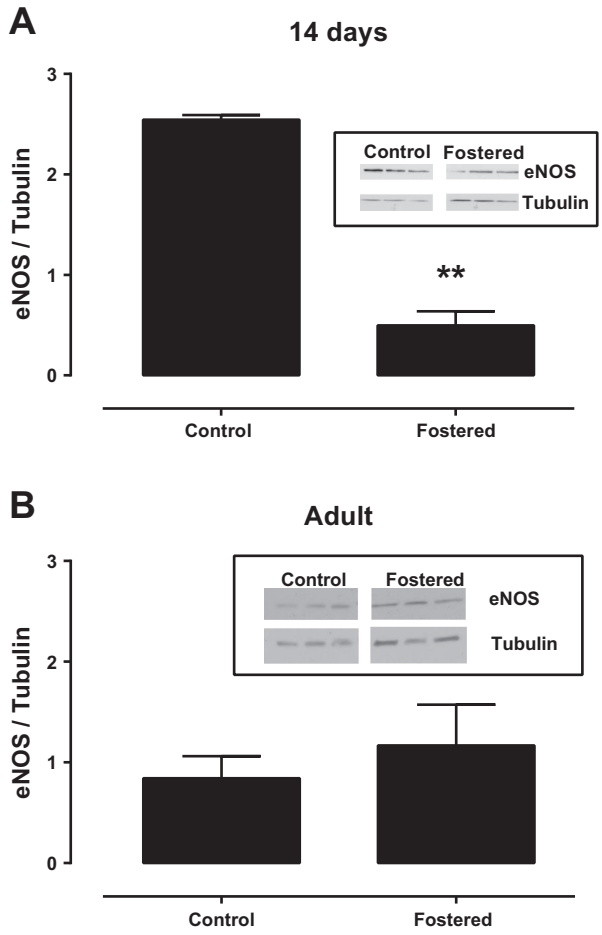

Fig. 7. Lung endothelial nitric oxide synthase (eNOS) expression. eNOS protein in lung endothelial cells of control and fostered 2-wk-old (*A*; $n = 3$ and 4, respectively) and adult (*B*; $n = 3$ for both groups) animals, normalized to tubulin expression. Representative Western blots are shown. All samples from control and cross-fostered animals were run on the same gel, and nonessential lanes were removed during image processing. $^{**}P < 0.01$ compared with samples of age-matched control animals by unpaired Student's *t*-test.

59, 60). AT_1 receptors modulate the ANG II-dependent pulmonary vasomotor tone. Inhibition of the AT_1 receptor in newborn pigs blunts the hypoxic pulmonary vasoconstriction response (12). In rats, the lung tissue AT_1 mRNA expression was reported by Morrell et al. (45) to be low early in life, whereas Gao et al. (28) showed that AT_1 receptor protein expression in the same tissue is highest during the fetal and neonatal period. This apparent discrepancy likely reflects the well-known lack of specificity of commercially available AT_1, AT_2, and Mas receptor antibodies (6). As such, in the present study, we chose instead to use RT-PCR to evaluate mRNA expression changes of the distinct RAAS pathway components.

ACE expression in the rat lung is developmentally regulated and lower in the newborn when compared with adult animals (64). Lung ACE activity has been developmentally studied in rodents and found to be low at birth and progressively increased with maturation (61). RAAS has been widely recognized as an important player in the pathobiology of adult-onset pulmonary arterial hypertension (2, 42, 55). Chronic hypoxia (36)- and monocrotaline (35)-induced pulmonary hypertension in adult rats is associated with a reduction in ACE activity. In the fetal period, the ACE activity changes associated with pulmonary hypertension have been studied. In the nitrofen-induced prenatal rat model of diaphragmatic hernia and pulmonary hypertension, the lung ACE activity increases when compared with control animals (10). A reduction in lung ACE protein expression, however, was documented in fetal mice subjected to hypoxemia (31), a noxious stimulus capable of inducing pulmonary hypertension (41). Together, these studies suggest that ACE expression and/or activity are susceptible to change during the fetal-neonatal period and may play a role in the pathogenesis of pulmonary hypertension. In the present study, the fostered pups' total lung tissue ACE mRNA expression was reduced at 1 wk but not 14 days of life. This finding suggests that the cross-fostering-induced decrease in ACE mRNA expression led to the upregulation of AT_1

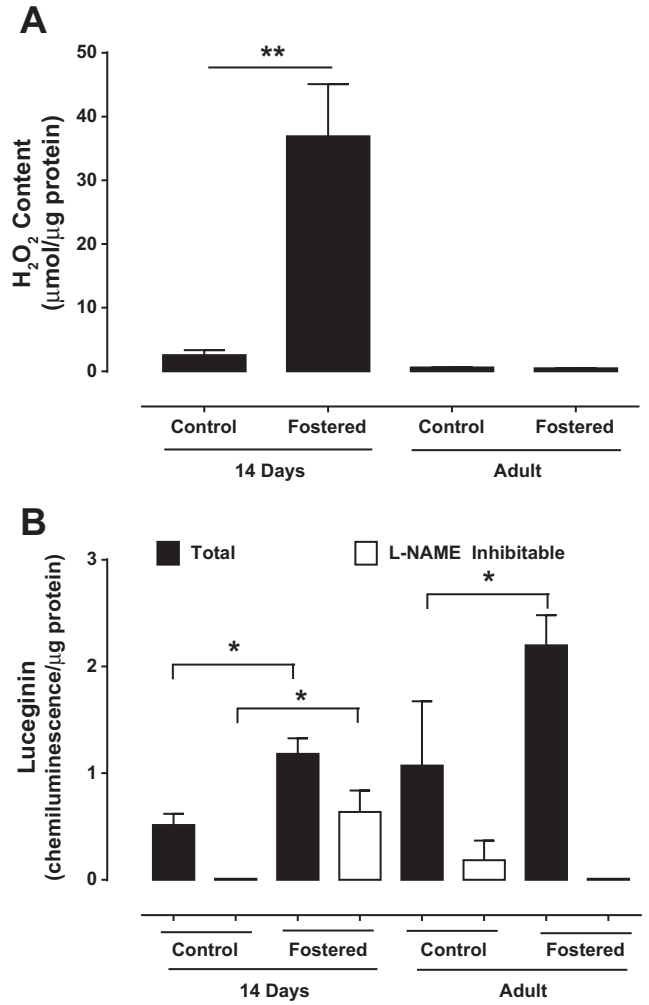

Fig. 8. Lung reactive oxygen species (ROS) generation. Control and fostered 2-wk-old and adult lung tissue ROS measured as polyethylene glycol-superoxide dismutase-inhibitable H_2O_2 content (*A*) and total and N^G-nitro-L-arginine methyl ester (L-NAME)-inhibitable lucigenin-dependent chemiluminescence (*B*). Both assays' data were normalized to tissue protein content. Means ± SE. *A*: 2-wk-old (control, $n = 4$; fostered, $n = 3$), adult (control, $n = 4$; fostered, $n = 4$). $^{**}P < 0.01$, compared with samples of age-matched control animals by unpaired Student's *t*-test. *B*: $n = 3$ for both ages and groups. $^{*}P < 0.05$ by 1-way ANOVA and multiple comparison testing.

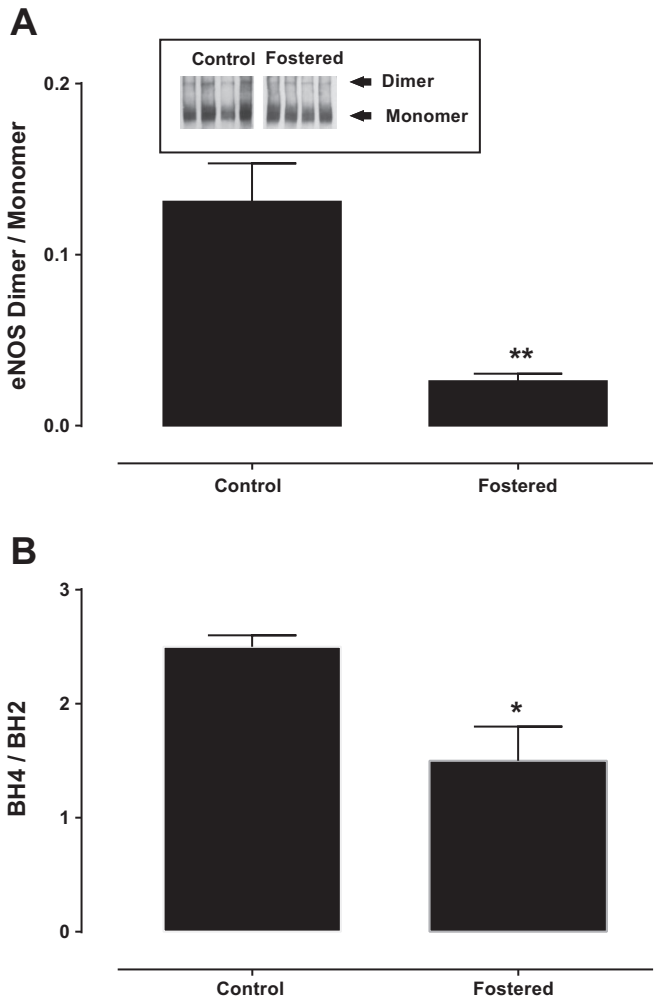

Fig. 9. Lung eNOS uncoupling and biopterin content. Control and fostered 2-wk old rat lung tissue eNOS dimer/monomer ratio (*A*; $n = 4$ for both groups) and tetrahydrobiopterin (BH4) and dihydrobiopterin (BH2) ratio (*B*; $n = 3$ for both groups). *A*, *inset*: Western blot is shown. All samples were run on the same gel, and nonessential lanes were removed during image processing. $*P < 0.05$ and $**P < 0.01$ compared with control samples by unpaired Student's *t*-test.

receptor expression at 14 days of age via reduction in lung ANG II content during the 1st wk of life.

It is interesting to note that although AT_1 receptor mRNA expression is increased in fostered animals at both 14 days of age and during adulthood when compared with controls, the pulmonary arteries' ANG II-induced force response is only enhanced later in life. This likely reflects the reduced lung AT_1 receptor expression documented by others during the neonatal period (45). Similarly, when compared with same-age control rats, the adult-fostered animals' enhanced pulmonary vasocontraction to U46619 is likely mediated via NOX-derived ROS generation. This is so, since adult-fostered animals exhibited upregulated expression of NOX isoforms, and incubation with the ROS scavenger Tempol abolished the enhanced, U46619-induced vasocontraction in fostered animals in a similar manner as reported by others (16).

It is known that ANG II induces endothelial dysfunction via a reduction in endothelial cell BH4 content, thus facilitating eNOS uncoupling and ROS generation (13, 29, 48, 53). BH4 is an essential cofactor for eNOS activity that is crucial for eNOS stabilization in its coupled form. BH4 is formed de novo via a GTP cyclohydrolase I pathway or via a DHFR enzyme-dependent alternative salvage pathway. Previous studies in rodents showed that in the presence of DHFR dysregulation, the resulting BH4 deficiency and BH2 accumulation lead to eNOS uncoupling and are associated with systemic hypertension (13, 17, 33). Thus the present-study data suggest that the pulmonary arterial eNOS uncoupling and ROS production in 14-day-old fostered animals were caused by a transient DHFR dysregulation.

In the present study, we documented that fostering-induced PV remodeling was present at 14 days of age and continued into adulthood (Fig. 4). Such changes have been reported in association with RAAS upregulation in adult animal models of pulmonary hypertension and ameliorated by AT_1 blockade (18). Following monocrotaline-induced pulmonary hypertension in adult rats, for instance, overexpression of Ang-(1–7) or

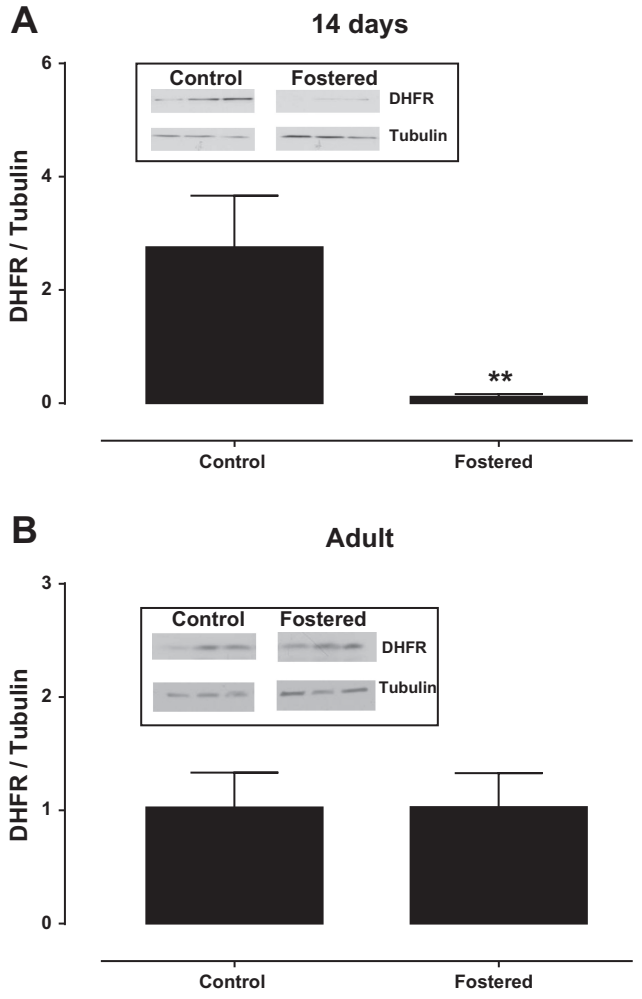

Fig. 10. Lung dihydrofolate reductase (DHFR) expression. Control and fostered 2-wk-old (*A*; $n = 4$ for both groups) and adult (*B*; $n = 3$ for both groups) lung endothelial cell DHFR protein normalized to tubulin expression. Representative Western blots are shown. All samples were run on the same gel and nonessential lanes removed during image processing. $**P < 0.01$ compared with samples of control animals by unpaired Student's *t*-test.

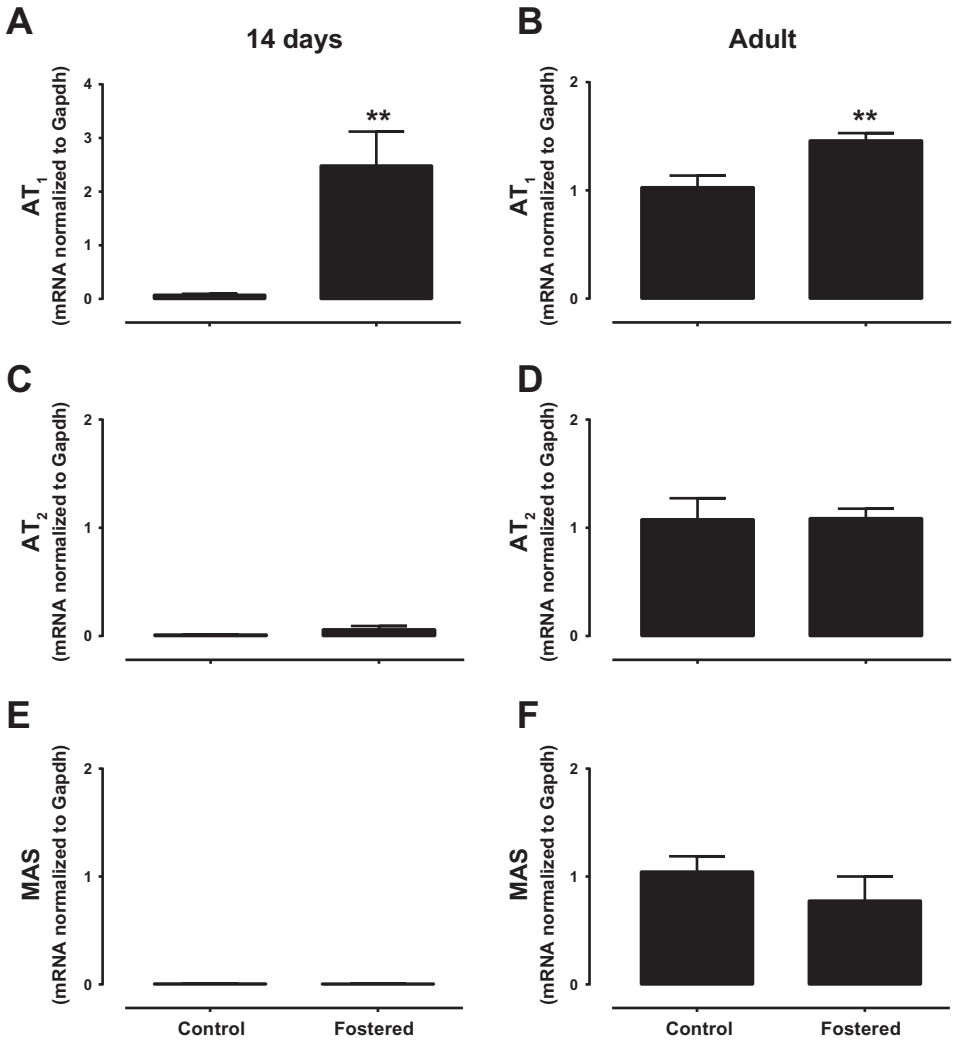

Fig. 11. ANG II receptor expression in the lung. Two-week-old (n = 3/group) and adult (n = 6/group) control and fostered lung tissue ANG II receptor types 1 (AT_1; *A* and *B*) and 2 (AT_2; *C* and *D*), and Mas (*E* and *F*) receptor mRNA, normalized to their respective mRNA GAPDH expression. Means ± SE. $^{**}P < 0.01$ compared with samples of age-matched control animals by unpaired Student's *t*-test.

ACE2 attenuates the PV remodeling process and reduces RV hypertrophy (54).

The extent to which the PV endothelial, mechanical, and histological changes documented in fostered pups are indicative of the presence of pulmonary hypertension in these animals merits further discussion. On one hand, the higher Fulton index values in experimental animals, when compared with control rats, suggest a fostering-induced PVR increase. Yet, we failed to confirm this finding by echocardiography, suggesting that if a group difference in PVR at either age is present, then the magnitude of PVR increase is small.

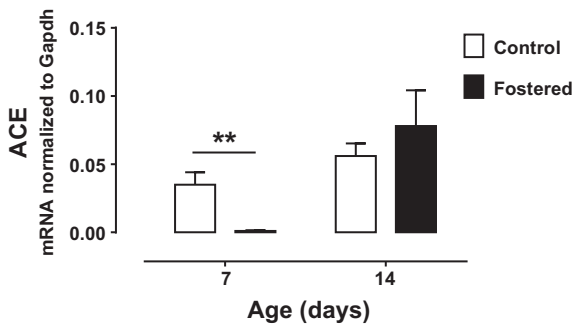

Fig. 12. Lung angiotensin-converting enzyme (ACE) expression. Control and fostered lung ACE mRNA normalized to their respective mRNA GAPDH expression at 7 and 14 days of life. $^{**}P < 0.01$ compared with samples of age-matched control animals by unpaired Student's *t*-test.

Nevertheless, the echocardiographic assessment of PVR relies on the PAAT and RVET measurements that are dependent on myocardial systolic performance. In fostered adult rats, TAPSE, an echocardiographic parameter of RV function (37), was abnormally decreased when compared with control animals (Fig. 3).

Reduced TAPSE heralds the presence of RV dysfunction in fostered adult rats. Others have shown that RV remodeling, associated with increased afterload, occurs not only in response to PVR rise but also following enhanced pulmonary arterial stiffness (56). Thus the echocardiographic evidence of reduced TAPSE in fostered adult animals, in the absence of a group difference in PVR index, can be explained as follows. Firstly, fostered animals exhibited PV remodeling that was likely associated with increased pulmonary arterial stiffness, thus possibly accounting for the reduced TAPSE values. Secondly, in the swine pulmonary hypertension model, a decrease in TAPSE values was shown to be present in the early-adaptive RV-remodeling phase before the onset of heart failure (1).

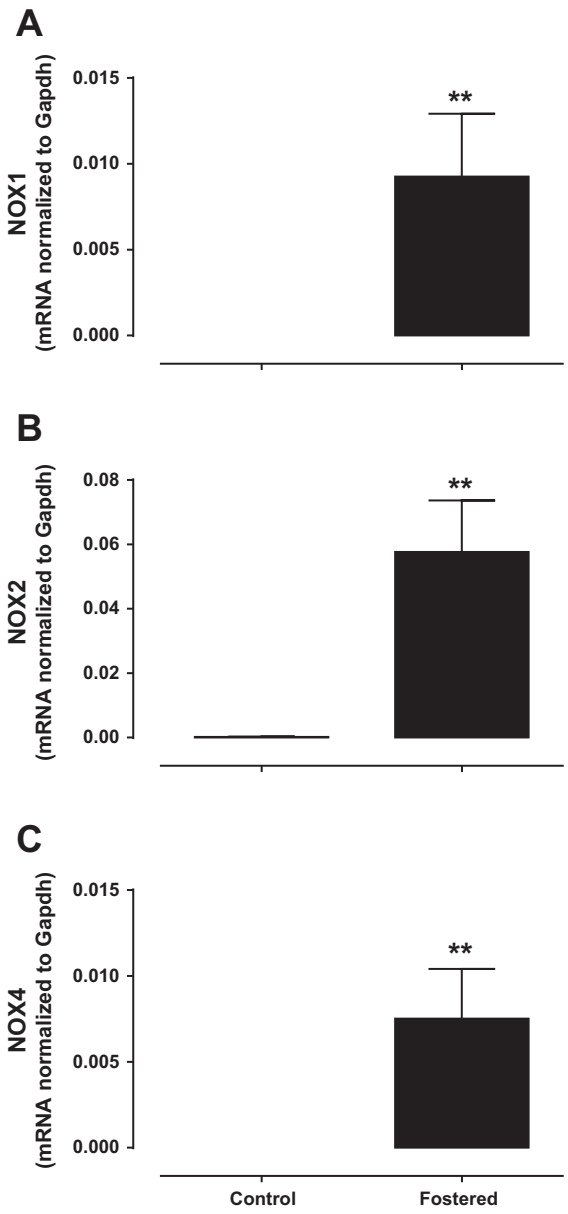

Fig. 13. Lung NADPH oxidase (NOX) expression. Adult control animals (n = 54) and fostered rats (n = 3) NOX isoforms 1 (*A*), 2 (*B*), and 4 (*C*) mRNA expression, normalized to their respective mRNA GAPDH expression. $^{**}P < 0.01$ compared with control data.

Lastly, in adult subjects with progressive pulmonary hypertension undergoing echocardiographic assessment, minimal increases in pulmonary arterial systolic pressure result in a significant decrease in TAPSE measurements (38). Taken together, the reduced TAPSE values documented in fostered adult rats, when compared with the control animals, are suggestive of a progressive increase in RV afterload without a significant rise in pulmonary arterial pressure at the time the measurements were obtained.

In summary, we demonstrated that cross-fostering interferes with the maternal-pup interaction and results in neonatal programming of PV changes. The mechanism involved in this process includes RAAS-mediated changes in the PV AT_1 receptor that promote endothelium dysfunction, ROS generation, and PV remodeling. Figure 14 outlines the pathways involved in the cross-fostering-induced PV changes.

The present findings have experimental and translational significance. Cross-fostering is commonly used to ensure adequate maternal milk supply when chronically subjecting newborn rodents to hypoxia (66) or hyperoxia (3) to induce pulmonary hypertension experimentally. The cross-fostering effects on the pulmonary vasculature ought to be distinguished from the chronic hypoxia/hyperoxia-induced pulmonary hypertension. Translationally, disturbance of the parental-newborn interaction is inevitable in infants requiring intensive care. The impact of parental-newborn disruption on the transition from fetal to neonatal life and the pathogenesis of PPHN merit further investigation.

GRANTS

Support for this work was funded by a grant from the Canadian Institutes of Health Research (MOP 133664; to J. Belik).

DISCLOSURES

No conflicts of interest, financial or otherwise, are declared by the authors.

AUTHOR CONTRIBUTIONS

Y.S. and J.B. conception and design of research; Y.S., S.S., J.P., and A.F.F. performed experiments; Y.S., S.S., J.P., A.J., A.F.F., P.J.M., and J.B. analyzed data; Y.S., J.P., A.J., P.J.M., and J.B. interpreted results of experiments; Y.S., S.S., and J.B. prepared figures; Y.S. and J.B. drafted manuscript; Y.S., A.J., P.J.M., and J.B. edited and revised manuscript; Y.S., S.S., J.P., A.J., A.F.F., P.J.M., and J.B. approved final version of manuscript.

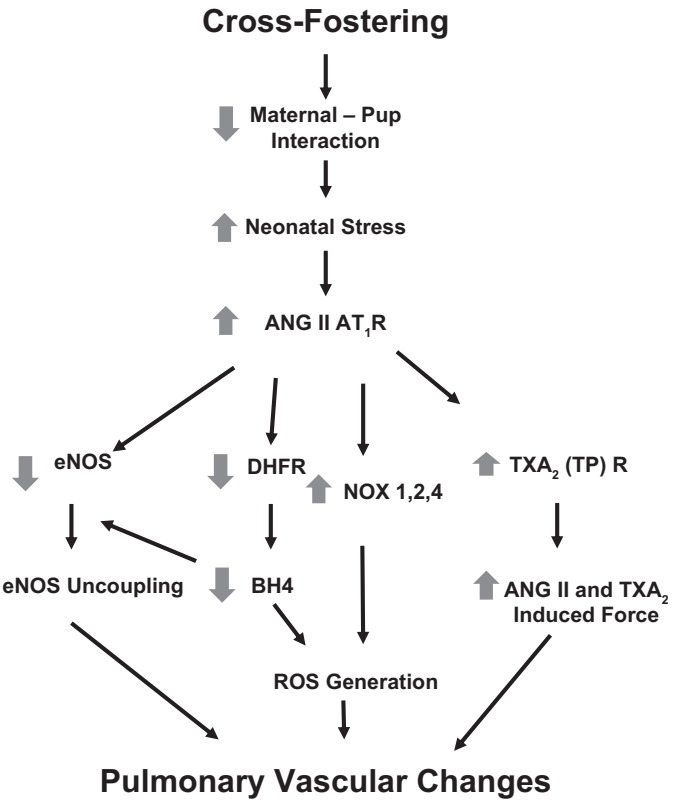

Fig. 14. Pathogenesis of fostering-induced PV changes. The diagram outlines the mechanism by which cross-fostering induces an increase in PVR during the neonatal period and adulthood. TXA_2 (TP) R, thromboxane A_2 receptor.

REFERENCES

1. **Aguero J, Ishikawa K, Hadri L, Santos-Gallego C, Fish K, Hammoudi N, Chaanine A, Torquato S, Naim C, Ibanez B.** Characterization of right ventricular remodeling and failure in a chronic pulmonary hypertension model. *Am J Physiol Heart Circ Physiol* 307: H1204–H1215, 2014.
2. **Antoniu SA.** Targeting RhoA/ROCK pathway in pulmonary arterial hypertension. *Expert Opin Ther Targets* 16: 355–363, 2012.
3. **Belik J, Jankov RP, Pan J, Yi M, Chaudhry I, Tanswell AK.** Chronic O2 exposure in the newborn rat results in decreased pulmonary arterial nitric oxide release and altered smooth muscle response to isoprostane. *J Appl Physiol* 96: 725–730, 2004.
4. **Belik J, McIntyre BA, Enomoto M, Pan J, Grasemann H, Vasquez-Vivar J.** Pulmonary hypertension in the newborn GTP cyclohydrolase I-deficient mouse. *Free Radic Biol Med* 51: 2227–2233, 2011.
5. **Belik J, Stevens D, Pan J, McIntyre BA, Kantores C, Ivanovska J, Xu EZ, Ibrahim C, Panama BK, Backx PH, McNamara PJ, Jankov RP.** Pulmonary vascular and cardiac effects of peroxynitrite decomposition in newborn rats. *Free Radic Biol Med* 49: 1306–1314, 2010.
6. **Benicky J, Hafko R, Sanchez-Lemus E, Aguilera G, Saavedra JM.** Six commercially available angiotensin II AT(1) receptor antibodies are nonspecific. *Cell Mol Neurobiol* 32: 1353–1365, 2012.
7. **Biagini G, Pich EM, Carani C, Marrama P, Agnati LF.** Postnatal maternal separation during the stress hyporesponsive period enhances the adrenocortical response to novelty in adult rats by affecting feedback regulation in the CA1 hippocampal field. *Int J Dev Neurosci* 16: 187–197, 1998.
8. **Bogdarina I, Welham S, King PJ, Burns SP, Clark AJ.** Epigenetic modification of the renin-angiotensin system in the fetal programming of hypertension. *Circ Res* 100: 520–526, 2007.
9. **Borgdorff MA, Koop AM, Bloks VW, Dickinson MG, Steendijk P, Sillje HH, van Wiechen MP, Berger RM, Bartelds B.** Clinical symptoms of right ventricular failure in experimental chronic pressure load are associated with progressive diastolic dysfunction. *J Mol Cell Cardiol* 79: 244–253, 2015.
10. **Bos AP, Sluiter W, Tenbrinck R, Kraak-Slee R, Tibboel D.** Angiotensin-converting enzyme activity is increased in lungs of rats with pulmonary hypoplasia and congenital diaphragmatic hernia. *Exp Lung Res* 21: 41–50, 1995.
11. **Broughton Pipkin F, Kirkpatrick SM, Lumbers ER, Mott JC.** Renin and angiotensin-like levels in foetal, new-born and adult sheep. *J Physiol* 241: 575–588, 1974.
12. **Camelo JS Jr, Hehre D, Devia C, Camelo SH, Bancalari E, Suguihara C.** The role of angiotensin II receptor-1 blockade in the hypoxic pulmonary vasoconstriction response in newborn piglets. *Neonatology* 93: 263–268, 2008.
13. **Chalupsky K, Cai H.** Endothelial dihydrofolate reductase: critical for nitric oxide bioavailability and role in angiotensin II uncoupling of endothelial nitric oxide synthase. *Proc Natl Acad Sci USA* 102: 9056–9061, 2005.
14. **Champagne FA, Meaney MJ.** Stress during gestation alters postpartum maternal care and the development of the offspring in a rodent model. *Biol Psychiatry* 59: 1227–1235, 2006.
15. **Champagne FA, Weaver IC, Diorio J, Dymov S, Szyf M, Meaney MJ.** Maternal care associated with methylation of the estrogen receptor-alpha1b promoter and estrogen receptor-alpha expression in the medial preoptic area of female offspring. *Endocrinology* 147: 2909–2915, 2006.
16. **Cogolludo A, Frazziano G, Cobeno L, Moreno L, Lodi F, Villamor E, Tamargo J, Perez-Vizcaino F.** Role of reactive oxygen species in Kv channel inhibition and vasoconstriction induced by TP receptor activation in rat pulmonary arteries. *Ann N Y Acad Sci* 1091: 41–51, 2006.
17. **Crabtree MJ, Channon KM.** Synthesis and recycling of tetrahydrobiopterin in endothelial function and vascular disease. *Nitric Oxide* 25: 81–88, 2011.
18. **de Man FS, Tu L, Handoko ML, Rain S, Ruiter G, Francois C, Schalij I, Dorfmuller P, Simonneau G, Fadel E, Perros F, Boonstra A, Postmus PE, van der Velden J, Vonk-Noordegraaf A, Humbert M, Eddahibi S, Guignabert C.** Dysregulated renin-angiotensin-aldosterone system contributes to pulmonary arterial hypertension. *Am J Respir Crit Care Med* 186: 780–789, 2012.
19. **Delaney C, Cornfield DN.** Risk factors for persistent pulmonary hypertension of the newborn. *Pulm Circ* 2: 15–20, 2012.
20. **Drukker A, Goldsmith DI, Spitzer A, Edelmann CM Jr, Blaufox MD.** The renin angiotensin system in newborn dogs: developmental patterns and response to acute saline loading. *Pediatr Res* 14: 304–307, 1980.
21. **Dumont FS, Kinkead R.** Neonatal stress and attenuation of the hypercapnic ventilatory response in adult male rats: the role of carotid chemoreceptors and baroreceptors. *Am J Physiol Regul Integr Comp Physiol* 299: R1279–R1289, 2010.
22. **Dunlop K, Gosal K, Kantores C, Ivanovska J, Dhaliwal R, Desjardins JF, Connelly KA, Jain A, McNamara PJ, Jankov RP.** Therapeutic hypercapnia prevents inhaled nitric oxide-induced right-ventricular systolic dysfunction in juvenile rats. *Free Radic Biol Med* 69: 35–49, 2014.
23. **Enomoto M, Jain A, Pan J, Shifrin Y, Van Vliet T, McNamara PJ, Jankov RP, Belik J.** Newborn rat response to single vs. combined cGMP-dependent pulmonary vasodilators. *Am J Physiol Lung Cell Mol Physiol* 306: L207–L215, 2014.
24. **Ferreira AJ, Santos RA, Raizada MK.** Angiotensin-(1–7)/angiotensin-converting enzyme 2/mas receptor axis and related mechanisms. *Int J Hypertens* 2012: 690785, 2012.
25. **Ferreira AJ, Shenoy V, Yamazato Y, Sriramula S, Francis J, Yuan L, Castellano RK, Ostrov DA, Oh SP, Katovich MJ, Raizada MK.** Evidence for angiotensin-converting enzyme 2 as a therapeutic target for the prevention of pulmonary hypertension. *Am J Respir Crit Care Med* 179: 1048–1054, 2009.
26. **Fornaro E, Li D, Pan J, Belik J.** Prenatal exposure to fluoxetine induces fetal pulmonary hypertension in the rat. *Am J Respir Crit Care Med* 176: 1035–1040, 2007.
27. **Francis DD, Champagne FA, Liu D, Meaney MJ.** Maternal care, gene expression, and the development of individual differences in stress reactivity. *Ann N Y Acad Sci* 896: 66–84, 1999.
28. **Gao J, Chao J, Parbhu KJ, Yu L, Xiao L, Gao F, Gao L.** Ontogeny of angiotensin type 2 and type 1 receptor expression in mice. *J Renin Angiotensin Aldosterone Syst* 13: 341–352, 2012.
29. **Gao L, Chalupsky K, Stefani E, Cai H.** Mechanistic insights into folic acid-dependent vascular protection: dihydrofolate reductase (DHFR)-mediated reduction in oxidant stress in endothelial cells and angiotensin II-infused mice: a novel HPLC-based fluorescent assay for DHFR activity. *J Mol Cell Cardiol* 47: 752–760, 2009.
30. **George ED, Bordner KA, Elwafi HM, Simen AA.** Maternal separation with early weaning: a novel mouse model of early life neglect. *BMC Neurosci* 11: 123, 2010.
31. **Goyal R, Leitzke A, Goyal D, Gheorghe CP, Longo LD.** Antenatal maternal hypoxic stress: adaptations in fetal lung renin-angiotensin system. *Reprod Sci* 18: 180–189, 2011.
32. **Hardziyenka M, Campian ME, de Bruin-Bon HA, Michel MC, Tan HL.** Sequence of echocardiographic changes during development of right ventricular failure in rat. *J Am Soc Echocardiogr* 19: 1272–1279, 2006.
33. **Harrison DG, Chen W, Dikalov S, Li L.** Regulation of endothelial cell tetrahydrobiopterin pathophysiological and therapeutic implications. *Adv Pharmacol* 60: 107–132, 2010.
34. **Ingelfinger JR, Nuyt AM.** Impact of fetal programming, birth weight, and infant feeding on later hypertension. *J Clin Hypertens (Greenwich)* 14: 365–371, 2012.
35. **Kay JM, Keane PM, Suyama KL, Gauthier D.** Angiotensin converting enzyme activity and evolution of pulmonary vascular disease in rats with monocrotaline pulmonary hypertension. *Thorax* 37: 88–96, 1982.
36. **Keane PM, Kay JM, Suyama KL, Gauthier D, Andrew K.** Lung angiotensin converting enzyme activity in rats with pulmonary hypertension. *Thorax* 37: 198–204, 1982.
37. **Kimura K, Daimon M, Morita H, Kawata T, Nakao T, Okano T, Lee SL, Takenaka K, Nagai R, Yatomi Y, Komuro I.** Evaluation of right ventricle by speckle tracking and conventional echocardiography in rats with right ventricular heart failure. *Int Heart J* 56: 349–353, 2015.
38. **López-Candales A, Lopez FR, Trivedi S, Elwing J.** Right ventricular ejection efficiency: a new echocardiographic measure of mechanical performance in chronic pulmonary hypertension. *Echocardiography* 31: 516–523, 2014.
39. **Loria AS, Pollock DM, Pollock JS.** Early life stress sensitizes rats to angiotensin II-induced hypertension and vascular inflammation in adult life. *Hypertension* 55: 494–499, 2010.
40. **Lu L, Mamiya T, Lu P, Niwa M, Mouri A, Zou LB, Nagai T, Hiramatsu M, Nabeshima T.** The long-lasting effects of cross-fostering on the emotional behavior in ICR mice. *Behav Brain Res* 198: 172–178, 2009.

41. **Luo ZC, Xiao L, Nuyt AM.** Mechanisms of developmental programming of the metabolic syndrome and related disorders. *World J Diabetes* 1: 89–98, 2010.
42. **Maron BA, Leopold JA.** The role of the renin-angiotensin-aldosterone system in the pathobiology of pulmonary arterial hypertension (2013 Grover Conference series). *Pulm Circ* 4: 200–210, 2014.
43. **Matthews PA, Samuelsson AM, Seed P, Pombo J, Oben JA, Poston L, Taylor PD.** Fostering in mice induces cardiovascular and metabolic dysfunction in adulthood. *J Physiol* 589: 3969–3981, 2011.
44. **Miyawaki M, Okutani T, Higuchi R, Yoshikawa N.** Plasma angiotensin II concentrations in the early neonatal period. *Arch Dis Child Fetal Neonatal Ed* 91: F359–F362, 2006.
45. **Morrell NW, Grieshaber SS, Danilov SM, Majack RA, Stenmark KR.** Developmental regulation of angiotensin converting enzyme and angiotensin type 1 receptor in the rat pulmonary circulation. *Am J Respir Cell Mol Biol* 14: 526–537, 1996.
46. **Nuyt AM.** Mechanisms underlying developmental programming of elevated blood pressure and vascular dysfunction: evidence from human studies and experimental animal models. *Clin Sci (Lond)* 114: 1–17, 2008.
47. **Nuyt AM, Alexander BT.** Developmental programming and hypertension. *Curr Opin Nephrol Hypertens* 18: 144–152, 2009.
48. **Oak JH, Cai H.** Attenuation of angiotensin II signaling recouples eNOS and inhibits nonendothelial NOX activity in diabetic mice. *Diabetes* 56: 118–126, 2007.
49. **Ognibene DT, Oliveira PR, Marins de Carvalho LC, Costa CA, Espinoza LA, Criddle DN, Tano T, Soares de MR, Resende AC.** Angiotensin II-mediated vasodilation is reduced in adult spontaneously hypertensive rats despite enhanced expression of AT2 receptors. *Clin Exp Pharmacol Physiol* 36: 12–19, 2009.
50. **Pernollet MG, Devynck MA, Macdonald GJ, Meyer P.** Plasma renin activity and adrenal angiotensin II receptors in fetal, newborn, adult and pregnant rabbits. *Biol Neonate* 36: 119–127, 1979.
51. **Pulgar VM, Yamashiro H, Rose JC, Moore LG.** Role of the AT2 receptor in modulating the angiotensin II contractile response of the uterine artery at mid-gestation. *J Renin Angiotensin Aldosterone Syst* 12: 176–183, 2011.
52. **Schinzari F, Tesauro M, Rovella V, Adamo A, Mores N, Cardillo C.** Coexistence of functional angiotensin II type 2 receptors mediating both vasoconstriction and vasodilation in humans. *J Hypertens* 29: 1743–1748, 2011.
53. **Seujange Y, Eiam-Ong S, Tirawatnapong T, Eiam-Ong S.** Role of angiotensin II on dihydrofolate reductase, GTP-cyclohydrolase 1 and nitric oxide synthase expressions in renal ischemia-reperfusion. *Am J Nephrol* 28: 692–700, 2008.
54. **Shenoy V, Ferreira AJ, Qi Y, Fraga-Silva RA, Diez-Freire C, Dooies A, Jun JY, Sriramula S, Mariappan N, Pourang D, Venugopal CS, Francis J, Reudelhuber T, Santos RA, Patel JM, Raizada MK, Katovich MJ.** The angiotensin-converting enzyme 2/angiogenesis-(1–7)/Mas axis confers cardiopulmonary protection against lung fibrosis and pulmonary hypertension. *Am J Respir Crit Care Med* 182: 1065–1072, 2010.
55. **Shenoy V, Qi Y, Katovich MJ, Raizada MK.** ACE2, a promising therapeutic target for pulmonary hypertension. *Curr Opin Pharmacol* 11: 150–155, 2011.
56. **Stevens GR, Garcia-Alvarez A, Sahni S, Garcia MJ, Fuster V, Sanz J.** RV dysfunction in pulmonary hypertension is independently related to pulmonary artery stiffness. *JACC Cardiovasc Imaging* 5: 378–387, 2012.
57. **Storme L, Aubry E, Rakza T, Houeijeh A, Debarge V, Tourneux P, Deruelle P, Pennaforte T; French Congenital Diaphragmatic Hernia Study Group.** Pathophysiology of persistent pulmonary hypertension of the newborn: impact of the perinatal environment. *Arch Cardiovasc Dis* 106: 169–177, 2013.
58. **van Vonderen JJ, Roest AA, Siew ML, Walther FJ, Hooper SB, te Pas AB.** Measuring physiological changes during the transition to life after birth. *Neonatology* 105: 230–242, 2014.
59. **Varga F, Sulyok E, Nemeth M, Tenyi I, Csaba IF, Gyori E.** Activity of the renin-angiotensin-aldosterone system in full-term newborn infants during the first week of life. *Acta Paediatr Acad Sci Hung* 22: 123–130, 1981.
60. **Velaphi SC, Despain K, Roy T, Rosenfeld CR.** The renin-angiotensin system in conscious newborn sheep: metabolic clearance rate and activity. *Pediatr Res* 61: 681–686, 2007.
61. **Wallace KB, Bailie MD, Hook JB.** Angiotensin-converting enzyme in developing lung and kidney. *Am J Physiol Regul Integr Comp Physiol* 234: R141–R145, 1978.
62. **Watkins AJ, Lucas ES, Torrens C, Cleal JK, Green L, Osmond C, Eckert JJ, Gray WP, Hanson MA, Fleming TP.** Maternal low-protein diet during mouse pre-implantation development induces vascular dysfunction and altered renin-angiotensin-system homeostasis in the offspring. *Br J Nutr* 103: 1762–1770, 2010.
63. **Weinmann A, Post M, Pan J, Rafi M, O'Connor DL, Unger S, Pencharz P, Belik J.** Tetrahydrobiopterin is present in high quantity in human milk and has a vasorelaxing effect on newborn rat mesenteric arteries. *Pediatr Res* 69: 325–329, 2011.
64. **Yosipiv IV, Dipp S, el-Dahr SS.** Ontogeny of somatic angiotensin-converting enzyme. *Hypertension* 23: 369–374, 1994.
65. **Yzydorczyk C, Gobeil F Jr, Cambonie G, Lahaie I, Le NL, Samarani S, Ahmad A, Lavoie JC, Oligny LL, Pladys P, Hardy P, Nuyt AM.** Exaggerated vasomotor response to ANG II in rats with fetal programming of hypertension associated with exposure to a low-protein diet during gestation. *Am J Physiol Regul Integr Comp Physiol* 291: R1060–R1068, 2006.
66. **Ziino AJ, Ivanovska J, Belcastro R, Kantores C, Xu EZ, Lau M, McNamara PJ, Tanswell AK, Jankov RP.** Effects of rho-kinase inhibition on pulmonary hypertension, lung growth, and structure in neonatal rats chronically exposed to hypoxia. *Pediatr Res* 67: 177–182, 2010.